



A NUMERICAL STUDY OF STRUCTURAL DAMAGE DETECTION USING CHANGES IN THE ROTATION OF MODE SHAPES

M. A.-B. ABDO AND M. HORI

Civil Engineering Department, The University of Tokyo, Japan. E-mails: abdo@eri.u-tokyo.ac.jp; hori@eri.u-tokyo.ac.jp

(Received 15 January 2001, and in final form 16 July 2001)

Damage detection using changes in global dynamic characteristics has been a hot research topic and attracted civil, aerospace, and mechanical engineering communities in recent years. In this paper, a numerical study of the relationship between damage characteristics and the changes in the dynamic properties is presented. It is found that the rotation of mode shape is a sensitive indicator of damage. The numerical results clarify that the rotation of mode shape has the characteristic of localization at the damaged region even though the displacement modes are not localized. Also, the results illustrate that the rotations of modes are robust in locating multiple damage locations with different sizes in a structure. Furthermore, using the changes in the rotation of mode shape does not need very fine grid of measurements to detect and locate damage, effectively.

© 2002 Elsevier Science Ltd.

1. INTRODUCTION

Structural systems are susceptible to structural damage over their lives due to many factors, such as, operating loads, fatigues, and corrosion. Undetected damage can result in the failure of the components of the structure, including fracture in tension or instability under compression, which are very costly in terms of human life and property damage. So, it is very essential and important to ensure the integrity and safety of structures [1]. Therefore, health monitoring of structures has been attracting much attention from civil, aerospace, and mechanical engineering communities in recent years.

Modal vibration test data, such as structural natural frequencies and mode shapes, can characterize the state of the structure [2]. Over the past three decades, detecting damage in a structure from changes in global dynamic properties has received considerable attention of civil, aerospace, and mechanical engineering communities. This is attributed to the fact that damage in the form of changes in the structural physical properties (i.e., stiffness, mass, and damping) will, in turn, alter the vibration properties of the structure such as, modal frequencies, mode shapes, and modal damping values. The change in the vibration properties can then be used as indicators of damage detection. Techniques of detecting damage in a structure by monitoring these changes have attracted much attention in recent years, and many approaches have been developed.

The use of the natural frequency and mode shape variations of a structure to determine global defects and deterioration has been investigated extensively [3–5]. Numerous studies have indicated that an increase in structural damage reflects a decrease in natural frequencies of the structure. Salawu [6] gave a literature review of the state of the art of

damage detection using changes in natural frequency. Actually, the changes in frequency imply the presence of crack or damage in a structure. However, determining the location of the crack, knowing the changes in the frequencies, is a completely different question. This is because, e.g., cracks at two different locations associated with certain crack length may cause the same amount of frequency change.

It was found that changes in the mode shapes of the structure were more sensitive indicators of damage than natural frequencies [7]. Yuen [8] showed that for a cantilever beam there was a systematic change in the first mode shape with respect to the damage location. He used finite element analysis to obtain the natural frequencies and the mode shapes of the damaged structure. Analyzing a beam, Pandey *et al.* [9] demonstrated the use of changes in the curvature mode shape to detect and locate damage. They also found that both the modal assurance criterion (MAC) [10] and the co-ordinate modal assurance criterion (COMAC) [11] were not sensitive enough to detect damage in its earlier stages. Chance *et al.* [12] found that measuring curvature directly (by measuring the strain) gave very improved results than the curvature calculated from the displacements. Also, Chen and Swamidass [13] found that strain mode shapes facilitated the location of a crack in a cantilever plate using finite element method simulation. Yam *et al.* [14] have found that the strain mode shape is more sensitive to structural local changes than the displacement mode shape. Quan and Weiguo [15] showed that for the steel deck of a bridge, the curvature mode shapes are the best among three damage recognition indices based on mode shapes (the COMAC, the flexibility, and the curvature mode shape). In addition, they found that some first vibration mode shapes, whatever vertical or horizontal modes, could be used equally to detect damage in the steel deck.

Indeed, it was difficult to measure the rotation of mode shapes in the past. So, most of the researchers have considered only the displacement mode shape as a reference to analyze the dynamic behaviour of the structures. However, in recent years, major advances have been realized in the field of structural dynamics and mechanical vibration measurements. The introduction of Scanning Laser Doppler Vibrometer (SLDV), has revolutionized dynamic testing and analysis due to its advantages such as its fast scanning capability and its non-contacting feature. Furthermore, the implementation of a six-degree-of-freedom dynamic data acquisition and visualization system currently is being developed [16]. Since the rotation of mode shapes may be feasible to be measured in the near future, the changes of rotation of mode shapes are investigated here to detect and locate structural damage.

The objective of this paper is to clarify the relationship between damage characteristics (location, size), and the changes in the rotation of the mode shapes. A careful numerical study is carried out by using the finite element method to analyze dynamic behaviour of damaged structural members. Furthermore, to examine the limitations of using this index to detect damage, several sets of coarser grids of measurements are used.

2. THEORY

2.1. ONE-DIMENSIONAL BAR

2.1.1. *Strain (slope) of mode shape*

For simplicity, we first consider a one-dimensional bar to study the change in the dynamic characteristics due to the presence of damage. The bar is simply supported. The length and cross-sectional area of the bar are L and A , and the Young's modulus and the density are E and ρ respectively. Damage is modelled as a loss in the Young's modulus by

ΔE , and the damaged zone is $x_d - h/2 < x < x_d + h/2$ with $h/L \ll 1$. The natural frequency ω and the corresponding displacement mode (u) are obtained by solving

$$c^2(x) \frac{\partial^2 u}{\partial x^2}(x) + \omega^2 u(x) = 0, \quad 0 < x < L, \tag{1}$$

$$u(x) = 0, \quad x = 0, L,$$

where $c^2 = (E - \Delta E)/\rho$ for $x_d - h/2 < x < x_d + h/2$ and $c^2 = E/\rho$ otherwise. If we expand ω as $\omega(h) \approx \omega + h\Delta\omega$ and u as $u(x, h) \approx u(x) + h\Delta u(x)$, it is well expected that $\omega(h)$ approaches ω and $u(x, h)$ approaches u as h goes to zero. However, if A is constant, strain ε does not admit such an expansion. The continuity of the stress at the intersection of undamaged and damaged parts, e.g., at $x_d - h/2$ leads to $E\varepsilon^l = (E - \Delta E)\varepsilon^r$. Here, superscript l or r indicates the left or the right of the intersection. The amount of strain discontinuity $[\varepsilon] = |\varepsilon^r - \varepsilon^l|$, is easily evaluated by approximating the above stress as $\sigma = E\varepsilon^0(x_d)$, where $\varepsilon^0(x_d)$ is the strain of the intact bar at x_d . That is

$$[\varepsilon] \approx \left(\frac{E}{E - \Delta E} - 1 \right) |\varepsilon^0(x_d)|. \tag{2}$$

It is of interest to mention that the strain here is the first derivative of the displacement mode, or the slope of the mode shape. In Figure 1, the first four modes of displacement and slope are plotted for a case of $L = A = 1$, and the damaged parameters are $\Delta E = 0.2E$, $h = 0.001L$, and $x_d = 0.6L$. Also, the first four modes of displacements and slope for the same characteristics of damage but at the middle of the bar, i.e., $x_d = 0.5L$ are plotted in Figure 2. In view of equation (2), we can expect that the change in the strain mode is more sensitive to the damage than the change in both the frequency and the displacement mode,

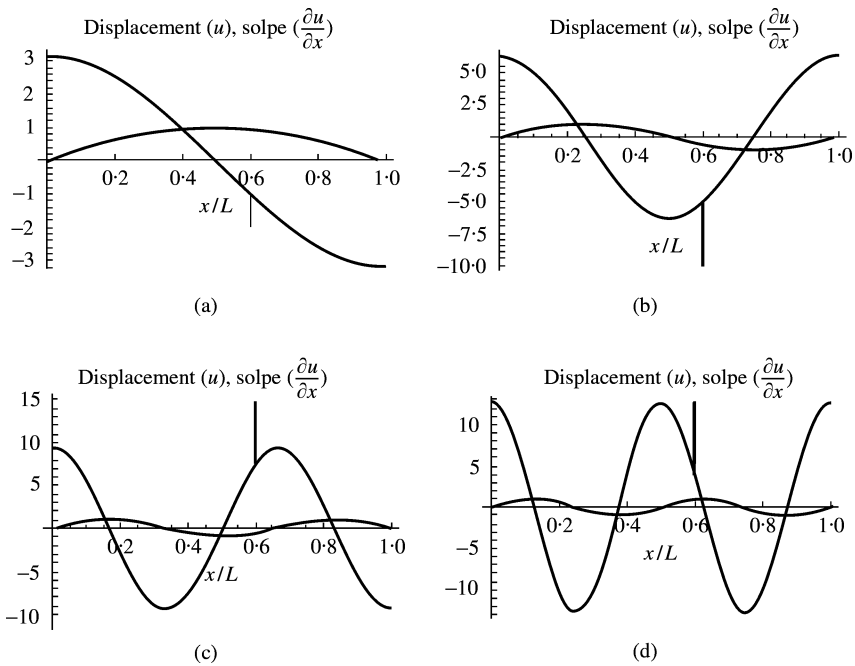


Figure 1. Displacement and slope of mode shapes of a bar element ($x_d = 0.6L$): (a) first mode; (b) second mode; (c) third mode; (d) fourth mode.

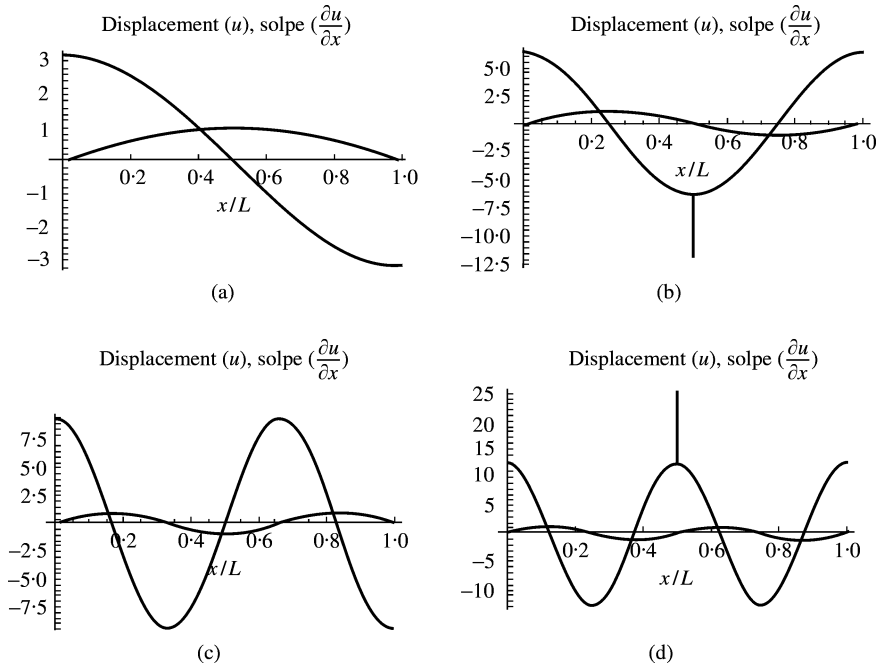


Figure 2. Displacement and slope of mode shapes of a bar element ($x_d = 0.5L$): (a) first mode; (b) second mode; (c) third mode; (d) fourth mode.

since the strain mode has a spike at the damage ($x = x_d$). The width of the spike is h and the height of the spike is related to ΔE ; the spike becomes sharper as h decreases and the height increases as ΔE increases. If $\varepsilon^0(x_d)$ is small, however, such a localized spike does not appear. These observations can be seen clearly in Figures 1 and 2. This suggests that we have to seek and use the more sensitive modes to detect damage throughout the bar.

2.1.2. Choice of the mode shapes

In Figures 1 and 2, almost all first four slopes of mode shapes can detect the damage except the first and third modes in Figure 2. This implies that these two modes are not sensitive to this damage. So, it is very important to find which modes to be used in damage detection. However, if all modes are used, the indication of damage may be masked by modes that are not sensitive to the damage. Since the change in the natural frequency of the mode i of a structure due to a localized damage is a function of the position vector of the damage, e.g., p and the reduction in stiffness caused by the damage ΔK [4], then

$$\Delta\omega_i = f(\Delta K, p). \tag{3}$$

Expanding this function about intact state ($\Delta K = 0$), and neglecting higher order terms, yields

$$\Delta\omega_i = f(0, p) + \Delta K \frac{\partial f}{\partial(\Delta K)}(0, p). \tag{4}$$

But $f(0, p) = 0$ for all p since there is no frequency change without damage. Hence,

$$\Delta\omega_i = \Delta K g_i(p). \tag{5}$$

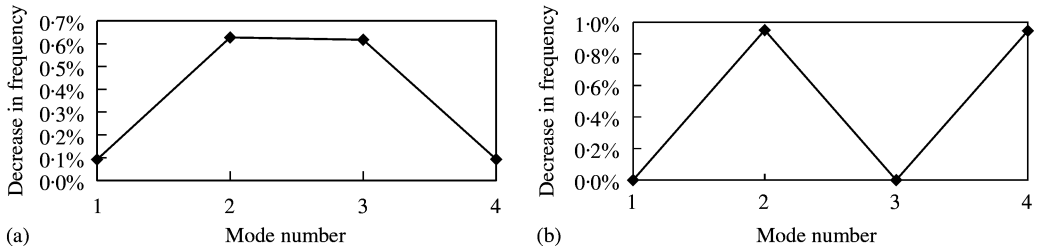


Figure 3. Changes in frequencies for the first four modes of a bar element: (a) $x_d = 0.6L$, (b) $x_d = 0.5L$.

From equation (5) it can be deduced that for the same amount of ΔK , modes that have higher changes in frequencies will have larger position vector and consequently, they are expected to be more sensitive to the existing damage. Figure 3(a) and (b) illustrates the changes in the natural frequencies of the first four modes of the bar element at $x_d = 0.6L$ and $x_d = 0.5L$ respectively. It is shown that higher changes in the natural frequencies indicate more localized strain modes at the damaged region and *vice versa*.

2.2. BEAM ELEMENT

In a similar manner, we consider a beam element to examine the above observations. The beam is simply supported, and has the stiffness $K = EI$ with E and I being the Young’s modulus and the second moment of the cross-section respectively. A narrow zone of damage is assumed at $x_d - h/2 < x < x_d + h/2$ with the stiffness $K - \Delta K$.

As h goes to zero, the natural frequency as well as the associated displacement, slope, bending moment, and shear force approach those of the intact beam. However, the curvature at the intersection suffers a jump; for instance, at $x_d - h/2$, the curvature satisfies $M + h\Delta M = K\kappa^l = (K - \Delta K)\kappa^r$, where κ and M stand for the curvature and bending moment. Again, by approximating M as $K\kappa^0(x_d)$, the jump of the curvature is evaluated as

$$[\kappa] \approx \left(\frac{K}{K - \Delta K} - 1 \right) |\kappa^0(x_d)|. \tag{6}$$

Since h is small, this jump leads to a spike in the curvature of mode shape, its height is related to ΔK and κ^0 . The above example of the beam element shows that the curvature mode shape is more suitable than the natural frequency and the displacement mode in detecting the location and the magnitude of damages. This emphasizes the observation that the derivatives of the mode shapes are localized and more sensitive than the displacement modes.

As a strain (slope) of mode shape is a good indicator of the bar, it is well expected that the rotations of mode shapes are good damage indicators for a plate member as well. We will examine this in detail, using the numerical computation in the next sections.

3. ANALYTICAL MODEL

As a practical example, the model chosen for this study is a steel plate. The background of this example is related to engineering applications in the construction of bridges, cranes, ships, etc. Since the stress concentration in the plate often occurs at the supported edges, the study of the dynamic stress concentration of a plate which suffers from failure at its

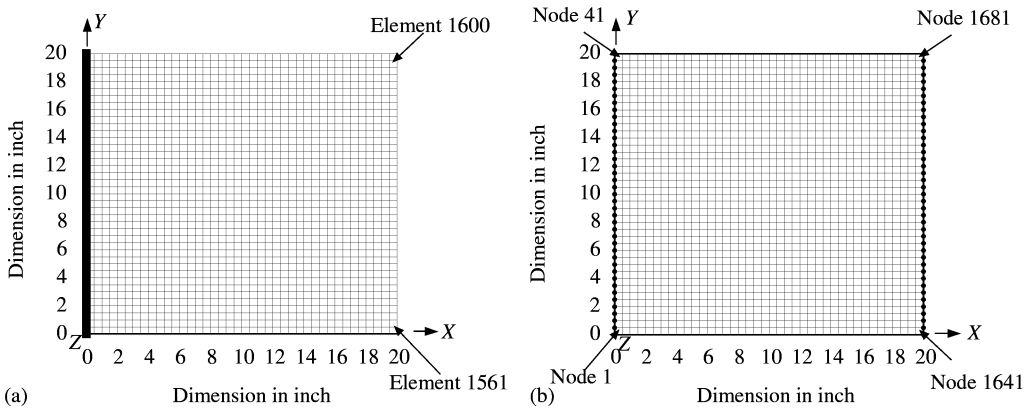


Figure 4. Finite element model of the steel plate: (a) cantilever plate: —■—, supported nodes; (b) simply supported plate: —●—, supported nodes.

TABLE 1
Damage characteristics of steel plate model

Damage characteristics	Cantilever plate (clamped, free, free, free)		Simply supported plate (simply, free, simply, free)	
	Case-I	Case-II	Case-I	Case-II
Number of damage(s)	1	2	2	2
Location of damage(s)	Middle	Ends	One edge only	Two edges
Damage size	10%	5 + 5%	2.5 + 7.5%	2.5 + 7.5%
Total amount of damage	10%	10%	10%	10%

connection(s) is of general significance. So, damage is mainly introduced at the supported edge(s) to represent the failure, e.g., in a welded connection of a structure.

The dimensions of the plate are 20 × 20 × 0.25 in, i.e., 508 × 508 × 6.35 mm and the mechanical properties of the plate are, Young’s modulus, $E = 210 \text{ GN/m}^2$, Poisson ratio, $\nu = 0.3$, and the density, $\rho = 7850 \text{ kg/m}^3$. Figure 4 illustrates the finite element model of the steel plate. The pre-damage and post-damage modal parameters were calculated numerically using the software package Marc/Mentat [17, 18]. Four-node shell element with six degrees of freedom (d.o.f.) per node, three translations and three rotations ($U_x, U_y, U_z, \theta_x, \theta_y, \theta_z$), are used. The convergence of the natural frequencies, displacement mode shapes and strain mode shapes were checked via comparison of different meshes and the finite element model consists of 40 × 40 elements, and 1681 nodes.

Two examples are studied to examine the effect of the boundary conditions; a cantilever and a simply supported plate, as shown in Figure 4. The first example is a cantilever plate which is clamped (all six d.o.f are restrained) at one edge, at $X = 0$ in and free otherwise. The second example is a plate which is simply supported (only the three translations, U_x, U_y, U_z , are restrained) at two edges, at $X = 0$ and 20 in and free otherwise. Table 1 shows the damage characteristics of the steel plate model. Actually, damage is mainly modelled as a part of free boundary at the damaged regions of the connection(s) of the plate, i.e., the damage is represented by free six d.o.f. at the damaged nodes.

The degree of damage (damage size) is related to the ratio between the length of the damaged region and the total length of the supported edge. For Case-I of the cantilever

plate, the three nodes 20, 21, and 22 at the middle of the clamped edge are set for damage, but for Case-II, the nodes 1, 2, 40, and 41 at the end of the clamped edge are set for damage. On the other hand, for Case-I of the simply supported plate, the damage is inflicted to one edge at nodes 1, 39, 40, and 41, but for Case-II, the damage is inflicted to both of the two supported edges simultaneously at nodes 1, 1679, 1680, and 1681. Indeed, two cases of damage are studied for each example to represent not only different locations but also different sizes. It is of interest to mention that for the cantilever plate, the damage is introduced symmetrically to the clamped edge to represent one or two damages with the same size, but for the simply supported plate the damage is introduced asymmetrically with damage ratio 1 : 3 to represent multiple damage locations with different sizes.

A further study was carried out to investigate an additional scenario of damage for the cantilever plate model. In this scenario, the change in the stiffness due to damage was modelled as a reduction in the modulus of elasticity (E) of two elements. Since this type of damage is not consistent with pre-mentioned scenarios of damages in the above examples, the results of this scenario are given in Appendix A. This additional scenario of damage confirms the generality and capability of damage detection method using the changes in the rotation of mode shape to detect and pinpoint different types of damage.

4. ANALYSIS OF RESULTS

The damage of the model in this study is assumed to affect only the stiffness matrix but not the inertia matrix in the eigenproblem formulation. This assumption is consistent with those used by Cawley and Adams [4], Yuen [8], and Pandey *et al.* [9]. Thus an eigenvalue problem of finding the natural frequencies and the displacement mode shapes is

$$(K - \lambda_i M)x_i = 0, \tag{7}$$

in which K and M are the stiffness and mass matrices of the intact structure, λ_i and x_i are the i th eigenvalue and displacement eigenvector of the intact structure respectively. However, when K is changed, equation (7) becomes

$$(K' - \lambda'_i M)x'_i = 0, \tag{8}$$

in which K' is the stiffness matrix of the damaged structure, λ'_i and x'_i are the i th eigenvalue and displacement eigenvector of the damaged structure respectively.

The eigenmodes calculated are orthogonal with respect to the inertia matrix M , i.e., $x_i^T M x_i = 1$. Since the rotation around Z-axis, θ_z , is very small for thin plates, only rotations around the X-axis, θ_x , and Y-axis, θ_y , are taken into consideration. These two rotations are normalized with respect to the square root of the sum of squares (SRSS). The maximum slope at any point of a thin plate can be calculated as [19]

$$\text{Maximum slope} = \sqrt{(\theta_x)^2 + (\theta_y)^2}. \tag{9}$$

So, for the sake of generality in this study, the following invariant is used for rotation at the j th node of the i th mode shape:

$$R_{ij} = \sqrt{(\theta_x)_{ij}^2 + (\theta_y)_{ij}^2}. \tag{10}$$

5. NUMERICAL RESULTS AND DISCUSSIONS

The first five frequencies and mode shapes for the intact and damaged plate are studied for the pre-mentioned two examples, cantilever and simply supported plate with 10% loss

TABLE 2

The percentage decrease in the natural frequencies due to 10% damage in the connection(s) of the model.

Mode number	Decrease in frequency (%)			
	Cantilever plate (clamped, free, free, free)		Simply supported plate (simply, free, simply, free)	
	Case-I	Case-II	Case-I	Case-II
1	0.4999	0.2767	0.0803	0.0803
2	0.0008	0.7762	0.4798	0.4798
3	0.2629	0.6421	0.5643	0.5625
4	0.2210	0.1214	0.1233	0.1267
5	0.0011	0.8706	0.4023	0.3988

in their connection(s). As mentioned before, these two examples represent different damage sizes and multiple damage locations. Furthermore, an additional scenario of damage is inflicted, as a 5% reduction in the modulus of elasticity (E), to both the elements 1561 and 1600. The results of this scenario are discussed in Appendix A.

5.1. NATURAL FREQUENCIES AND DISPLACEMENT MODE SHAPES

The percentage change in the first five natural frequencies of cantilever and simply supported plate for different cases of damage at the connection(s) of the plate model are shown in Table 2. It is clear from this table that there is a discernible change in the natural frequencies between the intact and damaged plate, but this does not give an indication of the location of damage. This is expected because natural frequencies represent the dynamic characteristics of the whole structure. However, it is important to mention that the decrements of natural frequencies are very small for the second and fifth modes in Case-I of the cantilever plate. This is attributed to the fact that these modes are antisymmetric modes (twisting modes), and consequently the node lines of these modes pass through the region of damage. The same thing can be said about the first and fourth modes in Case-II of the cantilever plate and both the cases of the simply supported plate, where the node lines pass through the damaged regions at the ends of the supported edges.

The absolute differences of the first displacement mode shapes between the intact and damaged cantilever plate for Case-I and Case-II are plotted in Figure 5(a) and (b) respectively. It can be easily seen that the damage cannot be located by the changes in the displacement modes. Similar results are obtained for the two cases of the simply supported plate. Again, this is because the lower modes are global in nature and hence will change globally even due to a local change such as failure at the connection(s).

5.2. ROTATION OF MODE SHAPES

The absolute differences of the first rotation of mode shapes between the intact and damaged cantilever plate for Case-I and Case-II are plotted in Figure 6(a) and (b) respectively. Similarly, the absolute differences of the first rotation of mode shapes for the two cases of the simply supported plate are plotted in Figure 7(a) and (b) respectively. From

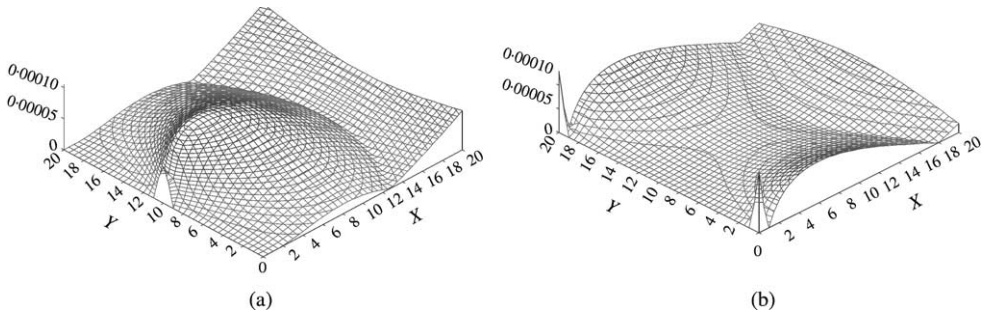


Figure 5. Absolute differences of the first displacement modes between the intact and damaged cantilever plate with 10% local failure: (a) Case-I; (b) Case-II.

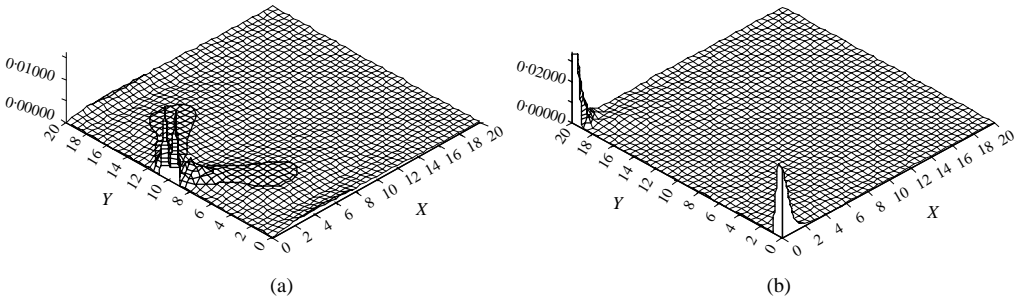


Figure 6. Absolute differences of the first rotation of mode shapes between the intact and damaged cantilever plate with 10% local failure: (a) Case-I; (b) Case-II.

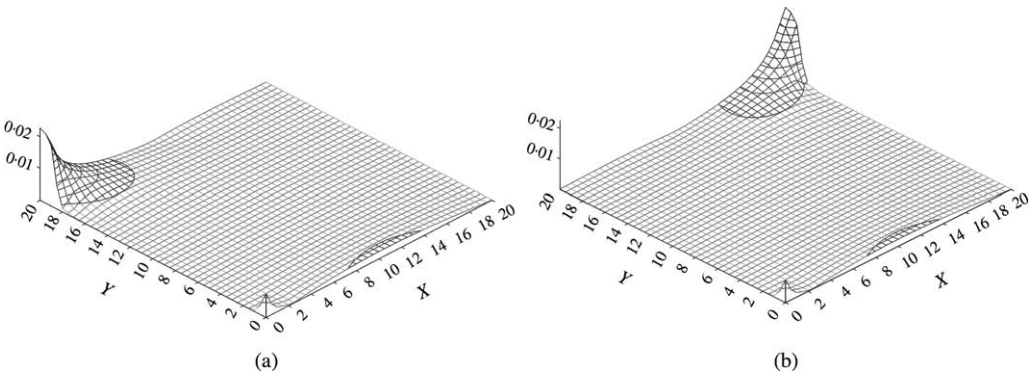


Figure 7. Absolute differences of the first rotation of mode shapes between the intact and damaged simply supported plate with 10% local failure: (a) Case-I; (b) Case-II.

these two figures, it can be easily seen that the rotations of mode shapes are localized at the damaged region for all cases of damage; one damage, two damages with the same size, and two damages with different damage sizes. It is important to mention that each component of the rotation, i.e., θ_x or θ_y , gives as good results as the invariant of rotation which is given in equation (10).

In the previous analysis, it was assumed that the mode shapes were known exactly on a very fine grid of measurements. But, in actual practice this will obviously not be the case.

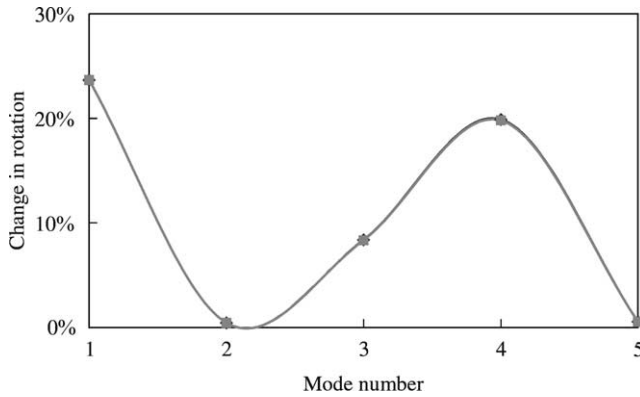


Figure 8. Changes in rotations of mode shapes for Case-I of the cantilever plate with different grids of measurements: —◆—, step $X = 0.5$ in, —■—, step $X = 2.0$ in.

So, reduced sets of data were used to determine how the results change using coarser grids of measurements. The step of measurements in the X direction is increased from 0.5 inch to 1.0 and 2.0 in, i.e., the measurements are reduced to approximately one-half and one-quarter respectively. Figure 8 shows the percentage change in rotation of mode shapes due to damage versus the mode number for Case-I of the cantilever plate. The change in rotation here is the absolute value of the ratio between the maximum difference in the rotation of mode shape due to damage and the maximum rotation of the intact case. Change of rotation can be written as

$$\text{Change in rotation} = \left| \frac{\text{Max}((R_{ij})_I - (R_{ij})_D)}{\text{Max} (R_{ij})_I} \right|, \quad (11)$$

where, $(R_{ij})_I$ and $(R_{ij})_D$ are the rotations at the j th node of the i th mode for the intact and damaged plate respectively. In Figure 8 it is noticed that the trend of changes in the rotation of mode shapes seems to be invariant with increase in the step of measurement in the X direction. Actually, this means that the rotation mode shape is stable and not so sensitive to the reduction in data of measurements in the X direction. This can be interpreted as the rotation of mode shape is measured directly and not calculated approximately from the displacement modes.

Also, it is observed that the trend of the changes in the rotation is in agreement with the trend of those changes in the natural frequencies. This proves that modes which have higher changes in natural frequencies are more sensitive to the damage and induce higher changes in the rotation of mode shape. Consequently, these modes are useful in determining the location of damage.

In the above analysis, it is assumed that the baseline for comparison is the intact case. To consider the extension of damage from a damaged plate to another severe damaged one, the changes in the rotation of modes for the cantilever plate are investigated. Figure 9 (a) and (b) shows the absolute differences of the first rotation of mode shapes (between the damaged cantilever plates with 10 and 20% local failure) for Case-I and Case-II respectively. This figure reflects the localization of rotational modes for the extension of damage, considering the less damaged plate as the baseline case. So, the above results indicate that changes in the rotation of mode shapes are effective and robust in detecting and locating both the initiation and extension of damage in a structure. Indeed, the usefulness of using changes in rotation of mode shapes is that they are localized at the damaged region and they have

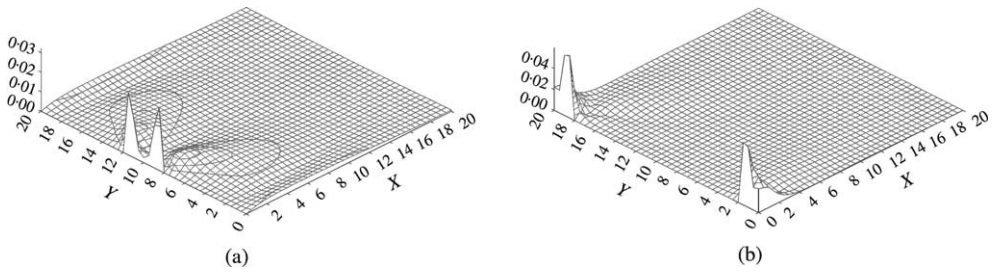


Figure 9. Absolute differences of the first rotation of mode shapes between the damaged cantilever plates with 10 and 20% local failure: (a) Case-I; (b) Case-II.

approximately zero values beyond the damaged region using only lower eigenmodes which can be easily measured experimentally. Even with only the first mode of the plate, i.e., the lowest frequency mode, the damage location can be accurately located.

6. SUMMARY AND CONCLUSIONS

Changes in the rotations of mode shapes due to the presence of structural damage, represented here in a numerical finite element model, have been investigated. The results of the steel plate model demonstrate the usefulness of the changes in the rotation of mode shape as a diagnostic parameter in detecting and locating damage in the connection(s) of the steel plate with different boundary conditions. It is shown that changes in the derivative (rotation or slope) of the mode shapes are more sensitive than the changes in the displacement mode shapes. Also, it is found that the rotation of mode is localized in the region of damage for initiation or extension of damage. The robustness in using changes in the above index is that it does not need higher modes of the structure to be used. Furthermore, this method has the ability to pinpoint a small amount of damage (5% reduction in the modulus of elasticity) in two small elements, as shown in Appendix A.

It is found that higher changes in the natural frequencies imply sensitive and more localized strain and rotation of modes at the damaged region. With a good choice of the mode shapes, the damage location can be accurately located even with only one mode of the structure, i.e., one of the lower frequency modes. On the other hand, it has also been shown that the rotation of mode shape is more stable beyond the damaged region and does not need fine grid of measurements for damage detection. Finally, due to the major advances in the fields of structural dynamics and experimental modal analysis, the rotation of mode shape is promising in detecting and locating damage in structures.

REFERENCES

1. J. B. KOSMATKA and J. M. RICLES 1999 *Journal of Structural Engineering, ASCE* **125**, 1384–1392. Damage detection in structures by modal vibration characterization.
2. D. J. EWINS 1984 *Modal Testing: Theory and Practice*. New York: Wiley, 313 pp.
3. R. D. ADAMS, P. CAWLEY, C. J. PYE and B. J. STORE 1978 *Journal of Mechanical Engineering Science* **20**, 93–100. A vibration technique for nondestructively assessing the integrity of structures.
4. P. CAWLEY and R. D. ADAMS 1979 *Journal of Strain Analysis* **14**, 49–57. The locations of defects in structures from measurements of natural frequencies.
5. D. F. MAZUREK and J. T. DEWOLF 1990 *Journal of Structural Engineering, American Society of Civil Engineers*, **116**, 2532–2549. Experimental study of bridge monitoring technique.

6. S. SALAWU 1997 *A Review, Engineering Structures* **19**, 718–723. Detection of structural damage through changes in frequency.
7. J. P. TANG and K. M. LEU 1991 *Journal of the Chinese Institute of Engineers* **14**, 531–536. Vibration tests and damage detection of P/C bridge.
8. M. M. F. YUEN 1985 *Journal of Sound and Vibration* **103**, 301–310. A numerical study of the eigenparameters of a damaged cantilever.
9. A. K. PANDEY, M. BISWAS, and M. M. SAMMAN 1991 *Journal of Sound and Vibration* **145**, 321–332. Damage detection from changes in curvature mode shapes.
10. T. WOLF and M. RICHARDSON 1989 *Proceedings of the Seventh International Modal Analysis Conference*, Vol. 1, 87–94. Las Vegas, Nevada, U.S.A. Fault detection in structures from changes in their modal parameters.
11. N. A. J. LIEVEN and D. J. EWINS 1988 *Proceedings of the Sixth International Modal Analysis Conference*, Vol. 1, 690–695. Hyatt Orlando, Kissimmee Florida, U.S.A. Spatial correlation of mode shapes, the co-ordinate modal assurance criterion (COMAC).
12. J. CHANCE, G. R. TOMLINSON and K. WORDEN 1994 *Proceedings of the 12th International Modal Analysis Conference*, 778–785. Honolulu, Hawaii, U.S.A. A simplified approach to the numerical and experimental modeling of the dynamics of a cracked beam.
13. Y. CHEN and A. S. J. SWAMIDAS 1994 *Proceedings of the 12th International Modal Analysis Conference*, 1155–1161. Honolulu, Hawaii, U.S.A. Dynamic characteristics and modal parameters of a plate with a small growing surface cracks.
14. L. H. YAM, T. P. LEUNG, D. B. LI and K. Z. XUE 1996 *Journal of Sound and Vibration* **191**, 251–260. Theoretical and experimental study of modal strain energy.
15. Q. QUAN and Z. WEIGUO 1998 *Proceedings of the 16th International Modal Analysis Conference*, Vol. 2, 945–951. Santa Barbara, California, U.S.A. Damage detection of suspension bridges.
16. C. E. WOON and L. D. MITCHEL 1996 *Proceedings of SPIE- The International Society for Optical Engineering*, Vol. 2868, 263–274. Ancona, Italy. Temperature-induced variations in structural dynamic characteristics: I—experimental.
17. MARC Analysis Research Corporation 1997 *Volumes: A, B, C*, Version K7.3.
18. MARC Analysis Research Corporation 1997 *Mentat User's Guide*, Version 3.3.
19. S. TIMOSHENKO and S. WOJNOWSKY-KRIEGER 1976 *Theory of Plates and Shells*. New York: McGraw-Hill Book Co., 580pp.

APPENDIX A: ADDITIONAL SIMULATION OF DAMAGE TO THE PLATE MODEL

A further study was carried out to investigate an additional scenario of damage for the cantilever plate model. The change in the stiffness due to damage was modelled as a reduction in the modulus of elasticity (E) of some elements. The damage is introduced as a 5% reduction in the modulus of elasticity of both elements 1561 and 1600, at the corner of the free edges, as shown in Figure 4. The reason for choosing these elements is that they are located at the free edge, i.e., they have very small stress and strain, which is opposite to the above scenarios of damages.

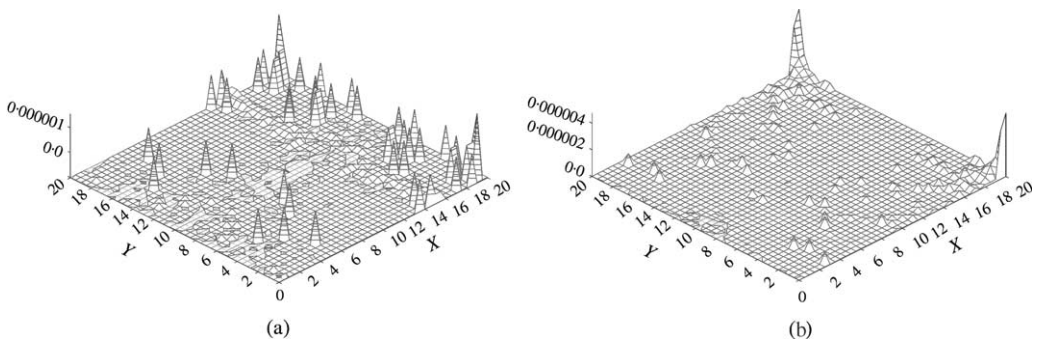


Figure A1. Absolute differences of the second mode between the intact and damaged (5% reduction in E in members 1561, 1600) cantilever plate: (a) displacement; (b) rotation.

Because the damage here is very small, the corresponding changes in the natural frequencies are as follows: 0.0002% for the second mode, 0.0006% for the fifth mode, and zero for the other modes. On the other hand, the changes in the displacement mode shapes are found to be zero for the first mode, and global for the other modes. This can be easily seen in Figure A1(a), which illustrates the absolute differences of the second displacement mode shape between the intact and the damaged (5% reduction in E in both elements 1561 and 1600), cantilever plate.

The changes in the rotations of mode shapes are found to localize at the damaged elements. Figure A1(b) illustrates the absolute differences of the second rotation of mode shape between the intact and the damaged cantilever plate. This additional scenario of damage emphasizes the generality and capability of the damage detection method using the changes in the rotation of mode shape to detect and to pinpoint different damage characteristics.